INTERNATIONAL SOCIETY FOR
SOIL MECHANICS AND
GEOTECHNICAL ENGINEERING

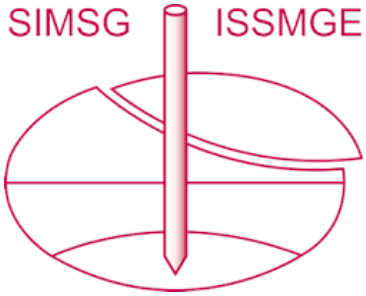

This paper was downloaded from the Online Library of the International Society for Soil Mechanics and Geotechnical Engineering (ISSMGE). The library is available here:

https://www.issmge.org/publications/online-library

This is an open-access database that archives thousands of papers published under the Auspices of the ISSMGE and maintained by the Innovation and Development Committee of ISSMGE.

Geotechnical and Geophysical Site Characterisation 5 – Lehane, Acosta-Martínez & Kelly (Eds)
© 2016 Australian Geomechanics Society, Sydney, Australia, ISBN 978-0-9946261-1-0

Reduced pressuremeter test time procedure and new analysis method

K. Iskander
Free University of Brussels ULB, Brussels, BEGIUM.

ABSTRACT: This paper presents solutions for the drawbacks of Pressuremeter Test (PMT) concerning the long time duration in site in comparison to the other in situ tests and the use of empirical rules to express the medium behavior. A new definition for pressure limit is adopted. It is determined within the first few loading steps. The proposed analysis accounts for: test rate, PMT size, volume of clay influenced by the test, heterogeneity of strain distribution around cavity. The medium behavior is being examined by the modified Cam Clay criterion. The medium octahedral shear stress strain relationship at the level of testing can be deduced. An overall clay medium shear modulus at some depth underground can be estimated. The present analysis method can be adopted for the design of tunnels and for modeling pile shaft clay medium interaction.

1 INTRODUCTION

Pressuremeter test requires long time duration in site compared to the necessary time to carry out the other in situ tests such as CPT and SPT. At any level underground, to determine the pressure limit that would be attained at infinite expansion of the cavity during testing, PMT requires at least twelve minutes. This duration differ from one test to another according to the considered code of practice. So for ten levels underground, PMT requires at least two hour time, while, for example CPT requires few minutes for testing along the same depth underground.

The reason for PMT long duration in site is the necessary time to determine the pressure limit ψ_L. Following French Standards NF P 94-110 (2000), P94-250-I (1996) and the ASTM D47 (1987), this conventional limit is defined by the pressure required to double the initial volume of the membrane cell. This limit has no solid theoretical bases and is assumed to express the clay failure state without defining a failure criterion. J.J. Powell (1990) and other authors separately reported the uncertainties in the methods of assessing and the applicability of pressure limit as well.

To avoid the drawbacks encountered in the analysis methods, Iskander (2013 &2015) adopted an energy concept taking into account: 1) Test rate: the developed excess pore pressure is sensitive to testing rate. Thus, the developed excess pore pressure during the test has to be measured to estimate the effective stress and introduce it in the analysis. 2) PMT size and type: the input energy is a function of the applied pressure and membrane volume. 3) Reliable analysis method: pressure limit $\psi_L$is newly defined by the applied pressure by PMT at the initiation of radial cracks at cavity surface that occur during the first few loading steps. These cracks are due to the negative stress development thereof. 4) The influenced clay volume during the test is obtained from the equality condition of input energy - work done across the influenced cylinder around PMT cavity. 5) Heterogeneity of strain distribution: to estimate the strains at any radius across the thickness of the influenced clay cylinder, that models the medium around the cavity, the plastic strain increment can be estimated by normality rule. These increments are assumed normal to the modified cam clay criterion (MCC) yield surface.

2 APPLICATION AND ANALYSIS

In two and three dimensional analysis for clay hollow cylinder that is assumed to simulate the clay medium around PMT probe. Iskander (2013& 2015) showed that at some pressure within the first three loading steps, during PMT, the developed excess pore water pressure at the inner radius surface became greater than the created increase in the compressive hoop stress. And, further loading increase by the probe results in further increase in the developed excess pore water pressure.

Moreover, it was shown that the effective octahedral stress path at the inner radius of hollow cylinder, that is the cavity radius, crosses the critical state boundary surface at this state of stress as well. This indicates that at this state of stress the clay fails thereof. Further, (Thevayanagam et al. 1994) and other authors observed the creation of radial cracks at the cavity surface during PMT which agrees with the results of the proposed analysis method. Thus, further loading results in increase in the developed negative stresses at the cavity surface and the corresponding strain increase is being due to the increase in the developed excess pore water pressure thereof.

In conclusion, cracks started to occur during the first three loading steps. It depends on test rate. The faster the test rate, the sooner the clay fails at the cavity surface. Further loading is time waste in site and more cost for nothing. Therefore, it is suggested to limit testing procedure to few loading steps.

The classical interpretation methods assume that the evolution of the strain of the perimeter of PMT cavity expresses the medium strains. But the heterogeneity of strain distribution around the cavity across the medium makes this assumption questionable. Iskander (2015) adopted the Modified Cam Clay criterion MCC (Roscoe & Burland 1968) and the variation energy principle Washizu (1975) to analyze the clay medium behavior due to cylindrical cavity expansion in three dimensions during PMT. Following MCC, the mean strains across the medium that correspond to the calculated average effective stresses can be estimated by normality rule (Equations are written in Appendix). So the increase in the work done by the developed average effective stresses increase and mean strains across the hollow cylinder must be equal to the input complementary energy by the probe so that:

$$V\Delta\psi/A = \frac{1}{2}\sum_{i=r}^{z} \bar{\epsilon}_i \times \Delta\bar{\sigma}'_i \qquad (1)$$

Where V= current membrane volume during an applied pressure increase of $\Delta\psi$; ψ = applied pressure by the probe; A = area of the hollow cylinder $\bar{\epsilon}'_{i,}$ $\Delta\bar{\sigma}'_i$ = mean strains, the increase in average effective stresses $\Delta\bar{\sigma}'_\theta$,$\Delta\,\bar{\sigma}'_R$ and $\Delta\bar{\sigma}'_z$ in hoop, radial and vertical directions across the influenced hollow cylinder.

2.1 Hollow cylinder test

Anderson & Pyrah (1987) performed tests on clay hollow cylinder of outer and inner radii of 7.5 and 1.25 cm and it was 15 cm high. This cylinder was provided by three piezometers at its mid height at 1.25, 3 and 5.5 cm measured from the axis of the cylinder. Clay Index properties were W_L = 42%, W_p = 23%, I_p= 19%, Activity = 0.63, Specific volume ν = 1.85. Critical State parameters λ = 0.136 and κ = 0.033. The reported test results are summarized in Tables 1& 2. for loading rates 30 kPa/minute and 10 kPa/minute respectively.

Figs 1-2 show that, during PMT, the developed excess pore water pressure increases as the test proceeds and the faster the test rate, the greater is the developed excess pore water pressure. But the developed excess pore water pressure decreases with distance from the axis of the cylinder.

Table 1 Experimental Test results, 30 kPa per minute

Applied pressure	Cavity radius	Developed excess pore water pressure at		
		Cavity	3 cm	5.5 cm
ψ kPa	a cm	u_a kPa	u_b kPa	u_c kPa
(1)	(2)	(3)	(4)	(5)
190	1.257	20	18	.1
220	1.27	40	36	4
250	1.29	80	58	10
280	1.32	120	76	16
310	1.37	140	87	23
340	1.41	160	96	30
370	1.45	180	102.	40

Table 2. Experimental Test results, 10 kPa per minute

Applied pressure	Cavity radius	Developed excess pore water pressure at		
		Cavity	3 cm	5.5 cm
ψ kPa	a cm	u_a kPa	u_b kPa	u_c kPa
(6)	(7)	(8)	(9)	(10)
160	1.252	15	10	5
210	1.261	35	18.9	9
240	1.282	60	31	10
260	1.299	75	37.8	16
290	1.317	95	52	19
320	1.37	110	63	27
360	1.454	120	68	40

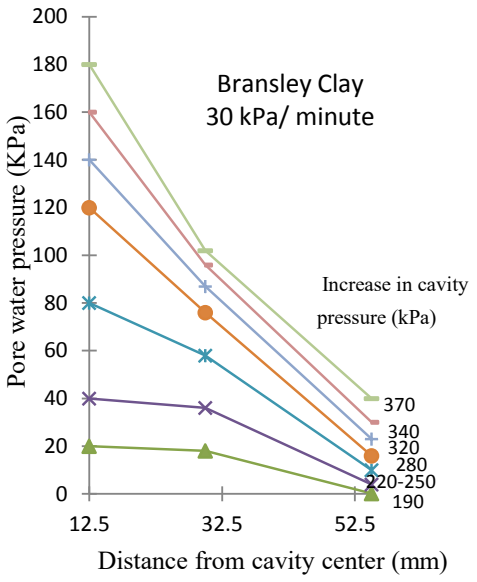

Fig 1. Pore pressure gradients across cylinder, 30 kPa / minute.

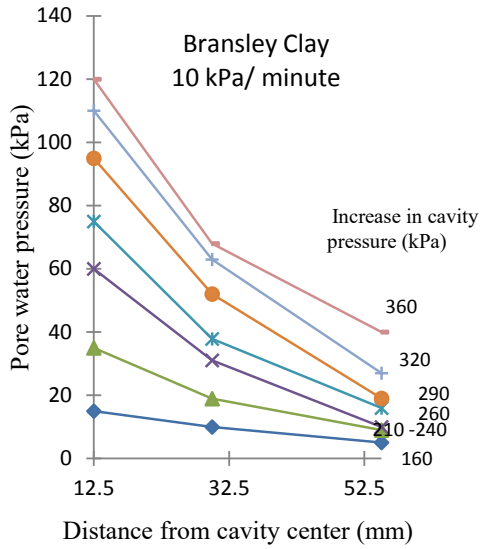

Fig 2. Pore pressure gradients across cylinder, 10 kPa/minute

2.2. Pressure limit ψ_L:

The average radial and hoop total stresses across the hollow cylinder at the PMT membrane mid height can be obtained by integrating the equations of Lamé (1852). To estimate the average effective stresses subtract the average measured developed excess pore water pressure. The vertical effective stress is equal to overburden pressure minus the average pore pressure. From equation (1), the deduced outer radii of the hollow cylinders that model the clay medium around the cavity during PMT and reported by Iskander (2015) are written in Tables 3 - 4 for the fast and slow testing rates respectively. Following Lamé (1852), the hoop stress at the inner radius of hollow cylinder is obtained as follows:

$$\sigma_{\theta a} = ((\psi - \sigma_h)R^2 + \psi\, a^2 - \sigma_h R^2)/(R^2 - a^2) \qquad (2)$$

Where σ_h= lateral stress at rest; R, a = outer and inner radii of hollow cylinder.

Table 3 shows for the faster test at the second loading step, the developed excess pore water pressure written in column (4) is equal to 40 kPa and is greater than the created compressive hoop stress at the cavity surface that is written in column (5). So, the total pressure limit = 220 then the effective pressure limit ψ'_L is equal to 180 kPa. The same analysis for the slower test rate showed that at the third loading step ψ_L= 240 kPa then ψ'_L= 180 kPa.

In the present work the deduced pressure limit is attained at the second and the third loading steps for fast and slow tests respectively and its effective value is independent of test rate.

Note the effective ψ'_L is more reliable than the total pressure limit for comparisons because the developed excess pore water pressure is sensitive to testing rate such as stated by Powell (1990).

Table 3 Hoop stress at cylinder inner radius 30 kPa/minute.

Applied pressure	Hollow cylinder radius		pore pressure at cavity	Hoop Stress
	inner	outer		
ψ kPa	a cm	R cm	u_a kPa	$\sigma_{\theta a}$ kPa
(1)	(2)	(3)	(4)	(5)
190	1.257	21.39	20	69.58
220	1.27	38.19	40	39.8
250	1.29	51.09	80	9.84
280	1.316	51.29	120	-20.26
310	1.368	60.69	140	-50.83
340	1.41	70.09	160	-80.17
370	1.45	79.89	180	-110.2

Table 4 Hoop stress at cylinder inner radius,10 kPa/minute.

Applied pressure	Hollow cylinder radius		pore pressure at cavity	Hoop Stress
	inner	outer		
ψ kPa	a cm	R cm	u_a kPa	$\sigma_{\theta a}$ kPa
(1)	(2)	(3)	(4)	(5)
160	1.252	18.96	15	99.74
210	1.261	26.66	35	49.64
240	1.282	41.76	60	19.79
260	1.299	43.86	75	-.228
290	1.317	48.56	95	-30.09
320	1.370	56.46	110	-60.22
360	1.454	73.66	120	-100.2

2.3. Octahedral shear stress $\bar{G}_{oct}$:

The geostatic stresses are the initial state of stress. The average effective stress in radial, in hoop and in vertical directions are written in Tables 5 – 6 for the fast and slow test rates respectively. The changes in octahedral stress deviators are estimated by Equation (3) so that:

$$\Delta\bar{\tau}_{oct} = \frac{1}{3}\left((\Delta\bar{\sigma}'_R - \Delta\bar{\sigma}'_\theta)^2 + (\Delta\bar{\sigma}'_\theta - \Delta\bar{\sigma}'_Z)^2 + (\Delta\bar{\sigma}'_Z - \Delta\bar{\sigma}'_R)^2\right)^{1/2} \qquad (3)$$

Where $\Delta\bar{\sigma}'_\theta$, $\Delta\,\bar{\sigma}'_R$ *and* $\Delta\bar{\sigma}'_z$: The change in average effective stresses in hoop, radial and vertical directions across the thickness of the hollow cylinder.

And, the corresponding change in strains are estimated following MCC from Equations (13-17) in Appendix. The octahedral change in strain deviator is estimated as follows:

$$\Delta\,\bar{\gamma}_{oct} = \frac{2}{3}\left((\Delta\bar{\epsilon}_R - \Delta\bar{\epsilon}_\theta)^2 + (\Delta\bar{\epsilon}_\theta - \Delta\bar{\epsilon}_z)^2 + (\Delta\bar{\epsilon}_z - \Delta\bar{\epsilon}_R)^2\right)^{1/2} \qquad (4)$$

Where $\Delta\bar{\epsilon}_\theta, \Delta\bar{\epsilon}_R$ *and* $\Delta\bar{\epsilon}_z$: The change in average radial, hoop and vertical strains across the thickness of the hollow cylinder respectively.

Accumulate the octahedral stress and strain change values for the successive hollow cylinders that model the whole medium. The medium average shear modulus at the level of the test is defined by $\bar{\tau}_{oct}/\bar{\gamma}_{oct}$. (5)

Table 5. Octahedral effective stress strain relationship, 30 kPa per minute.

Hollow Cylinder radius		Average Effective Stress			Average Octahedral	
Outer	Inner	Radial	Hoop	Vertical	Stress	Strain
R	a	$\bar{\sigma}'_R$	$\bar{\sigma}'_\theta$	$\bar{\sigma}'_Z$	$\bar{\tau}_{oct}$	$\bar{\gamma}_{oct}$
cm	cm	kPa	kPa	kPa	kPa	%
(1)	(2)	(3)	(4)	(5)	(6)	(7)
24.29	1.257	1.90	4.33	1.05	2.57	0.10
42.29	1.270	1.64	0.82	1.31	0.33	0.01
48.29	1.290	2.60	3.61	03.1	0.41	0.02
54.29	1.316	2.60	3.46	3.03	0.35	0.01
60.29	1.368	3.02	3.91	3.46	0.36	0.01
62.29	1.410	2.97	4.02	3.49	0.43	0.02
66.29	1.450	4.37	5.65	5.00	0.52	0.02

Table 6. Octahedral effective stress strain relationship 10 kPa per minute.

Hollow Cylinder radius		Average Effective Stress			Average Octahedral	
Outer	Inner	Radial	Hoop	Vertical	Stress	Strain
R	a	$\Delta\bar{\sigma}'_R$	$\Delta\bar{\sigma}'_\theta$	$\Delta\bar{\sigma}'_Z$	$\bar{\tau}_{oct}$	$\bar{\gamma}_{oct}$
cm	cm	kPa	kPa	kPa	kPa	%
(1)	(2)	(3)	(4)	(5)	(6)	(7)
20.26	1.252	1.2	4.92	2.95	1.52	0.06
36.26	1.2614	0.89	2.73	1.82	0.75	0.03
40.26	1.282	- 0.09	1.35	0.61	0.59	0.02
42.26	1.299	2.55	3.55	3.04	0.41	0.02
58.26	1.317	1.71	0.95	1.38	1.18	0.05
62.26	1.37	3.34	4.75	4.03	0.58	0.02
66.26	1.454	5.40	7.67	6.50	0.93	0.03

The results are plotted in Fig 3 for fast and slow test rates. It shows the evolution of medium octahedral shear stress and strain until failure following MCC criterion. In the present work, the medium shear modulus value is found independent of test rate. The value of average octahedral shear modulus $\bar{G}_{oct}$ is found = 2640 and 2600 kPa for the fast and slow test rates. Note the present analysis method is valid for linear and nonlinear stress strain relationships as well.
Applying the present analysis method at different depths under the ground, the shear modulus variation with depth can be found and an overall shear modulus across some depth in question can be estimated.

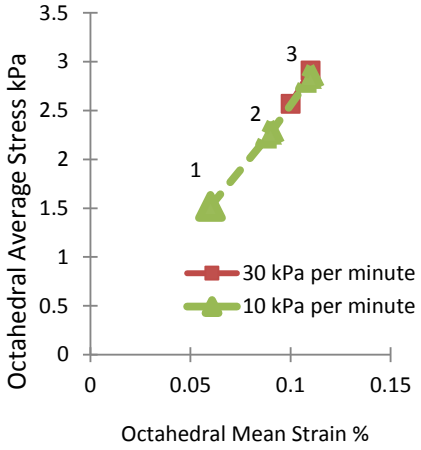

Fig 3. Octahedral Stress Strain Relationship

3 SUMMARY AND CONCLUSIONS

a) MCC and the variation energy principal are adopted to examine the clay medium behavior due to cavity expansion during the PMT.
b) The outer radius of clay hollow cylinder influenced and models the medium around PMT cavity can be deduced.
c) A proposed new pressure limit is defined by the applied pressure that initiate radial cracks at the cavity surface during PMT.
d) The analysis of the hollow cylinder test results showed that the deduced effective limit pressure is independent of test rate and the medium average octahedral shear modulus at the level of testing as well.
e) The present analysis method is devoted to analyze the normally consolidated clay under undrained conditions. It can be adopted to analyze soil behavior under drained conditions.
f) The present analysis method is applicable for the design of tunnels and piles.
g) It is suggested to provide PMT probe by two piezometers, one at the membrane cell, the other in the soil against the first one at short distance far from it but both at the membrane cell mid height.
h) More test data is required to confirm the conclusions and to analyze other applications in geotechnical design.

4 APPENDIX

4.1 The derived equations to calculate the strains

The average values of the total hoop and radial stresses across the thickness of hollow cylinder of outer and inner radii R and a are expressed as follows:

$$\bar{\sigma}_\theta = \frac{(\psi a - \sigma_h R)}{(R-a)} \qquad (6)$$

$$\bar{\sigma}_R = -\frac{(\psi a + \sigma_h R)}{(R+a)} \quad (7)$$

$\bar{\sigma}_Z = \gamma z$, the overburden pressure (8)

Where ψ = the applied pressure by the probe, R = outer radius of clay hollow cylinder, a = radius of the cavity radius that is the radius of membrane cell at its mid height,

The corresponding average effective stresses are:

$\bar{\sigma}'_\theta = \bar{\sigma}_\theta - \bar{u}$ (9)

$\bar{\sigma}'_R = \bar{\sigma}_R - \bar{u}$ (10)

$\bar{\sigma}'_Z = \bar{\sigma}_Z - \bar{u}$ (11)

Where $\bar{u}$ the average developed excess pore water pressure across the thickness of hollow cylinder.

The modified Cam Clay (MCC) expressed in terms of (p', J, θ_L) so that:

$$F = \frac{J^2}{(p' g(\theta_L))^2} - \frac{p'_0}{p'} + 1 = 0 \quad (12)$$

Where p' = the current mean effective stress; p'_0 = the initial mean effective stress and $=(\sigma'_h + \sigma'_z)/3$; $J = \sqrt{J_2}$; J_2= second deviator stress invariant defined by $\left(\bar{S}'^2_R + \bar{S}'^2_\theta + \bar{S}'^2_Z\right)/2$; $\bar{S}'_R$,$\bar{S}'_\theta$and $\bar{S}'_z$ are the three deviator normal stresses $\bar{S}'_R = (\bar{\sigma}'_R - p')$, $\bar{S}'_\theta = (\bar{\sigma}'_\theta - p')$ and $\bar{S}'_Z = (\bar{\sigma}'_Z - p')$; Lode angle $\theta_L = \frac{1}{3}\sin^{-1} - \frac{J_3}{2}\left(\frac{3}{J_2}\right)^{1.5}$; J_3 = third deviator of stress = $\left(\bar{S}'^3_R + \bar{S}'^3_\theta + \bar{S}'^3_Z\right)/3$ and,

$$g(\theta_L) = \frac{\sin\phi'_{cs}}{\cos\theta_L + \frac{(\sin\phi'_{cs}\sin\theta_L)}{\sqrt{3}}} \quad (13)$$

Where ϕ'_{cs}= the critical state angle of shearing resistance.

From normality in the π plane the strain increase is given by the chain rule so that;

$$\bar{\epsilon}_i = \frac{\partial F}{\partial J}\frac{\partial J}{\partial \bar{\sigma}_i} + \frac{\partial F}{\partial \theta_L}\frac{\partial \theta_L}{\partial \bar{\sigma}_i} \quad (14)$$

$$Where: \frac{\partial F}{\partial J} = \frac{2J}{\left(p' g(\theta_L)\right)^2} \quad (15)$$

$$\frac{\partial F}{\partial \theta_L} = \frac{2J^2}{p'^2 g(\theta_L)} \frac{\left(\cos\theta_L \sin\phi'_{cs}\right)/\sqrt{3} - \sin 3\theta_L}{\sin\phi'_{cs}} \quad (16)$$

Hereafter the stress partial differentials for $\bar{\sigma}'_R$ and the others by cyclic rotation

$$\frac{\partial J}{\partial \bar{\sigma}'_R} = \frac{\bar{S}'_R}{2\sqrt{2}J} \quad (17)$$

$$\frac{\partial \theta_L}{\partial \bar{\sigma}'_R} = \frac{-\sqrt{3}(2\bar{S}'^2_R - \bar{S}'^2_\theta - \bar{S}'^2_z) + 3\sqrt{J_2}\bar{S}'_R \sin 3\theta_L}{3\sqrt{4J_2^3 - 27J_3^2}} \quad (18)$$

4.2 The proposed two piezometer pressuremeter test device (PCT/BE2011/000026; EP 0705941A1):

Description

The two piezometer PMT consists of two separate parts: (1) the standard PMT probe equipped by a piezometer at its membrane cell mid height; and (2) a separate and movable part that is a short tube of smaller diameter than the intermediary between the ground surface and the probe membrane cell. This tube contains an inclined gun. The ball of this gun is a hypodermic needle that measures pore water pressure.

Device installation

After installing the standard PMT under the ground, the tube of the second movable part is to be introduced. The hypodermic needle is inserted by shooting it into the ground in inclined direction, almost 35 cm to reach from just above the expanding membrane to a point opposite the present piezometer in the membrane cell but at short distance far from it.

After carrying out the test, the hypodermic needle is to be pulled back to its initial position in the gun. Then the tube that contains the gun is pulled up to the ground surface. This procedure is to be repeated at each level of testing.

5 REFERENCES

AFNOR. (1996).”French Standard NF P 94-250-1”, Eurocode 7 Calcul géotechnique.

AFNOR. (2000). ”French Standard NF P 94-110”, Essai pressiométrique Ménard.

Anderson, W., Pyrah, I.C., and Ali, F. (1987). “Rate Effects in Pressuremeter test in Clays.” Journal of geotechnical Engineering. ASCE. 113(11), 1348-1358.

ASTM standard D4719-87, “Standard test method for Pressuremeter testing in soils”, Annual book of ASTM standards, vol. 04.08 American Society for testing materials.

Iskander, K. (2013). “New Pressuremeter test analysis based on critical state mechanics.” International journal of geomechanics, 10.1061 (ASCE) , GM.1943-5622.0000257.

Iskander, K. (2015). “Three Dimensional Cavity expansion analysis for strain heterogeneity in clay medium by Pressuremeter test results,” ISP7-Pressio, International symposium 60 years of pressuremeters in Tunisia, pp 121-135.

Lamé, G. (1852). ”Leçons sur la théorie mathématique de l’élasticité des corps solides” Bachelier, Paris.

Powel, J. J. M. (1990). “A comparison of four different PMTs and their methods of interpretation in a stiff heavily overconsolidated clay.” Proceedings of the Third International Symposium on Pressuremeters, Oxford.

Roscoe, K.H., and Burland, J.B. (1968). “On the generalized stress strain behavior of wet clays Engineering plasticity.” (Ets. J Heyman and F. Leckie) 535-609 Cambridge University Press.

Thevayanagam, S.L., Chameau, J.L., and Altschaeffl, A.G. (1994). “Some Aspects of Pressuremeter test interpretation in clay” Géotechnique vol. 44 (2),319-334.

Washizu, K. (1975). “Variational Methods in Elasticity and Plasticity”. Publisher Pergamon Press.